Rules governing metal coordination in clusters from Aβ-Zn(II) complexes from quantum mechanical calculations

Supplementary information

Julen Aduriz-Arrizabalaga, Jose M. Mercero, David de Sancho, and Xabier Lopez
Polimero eta Material Aurreratuak: Fisika, Kimika eta Teknologia, Kimika Fakultatea, UPV/EHU Donostia International Physics Center (DIPC), PK 1072, 20018 Donostia-San Sebastian, Euskadi, Spain
(Dated: September 29, 2023)

I. PERFORMANCE OF THE DIFFERENT DFT FUNCTIONALS

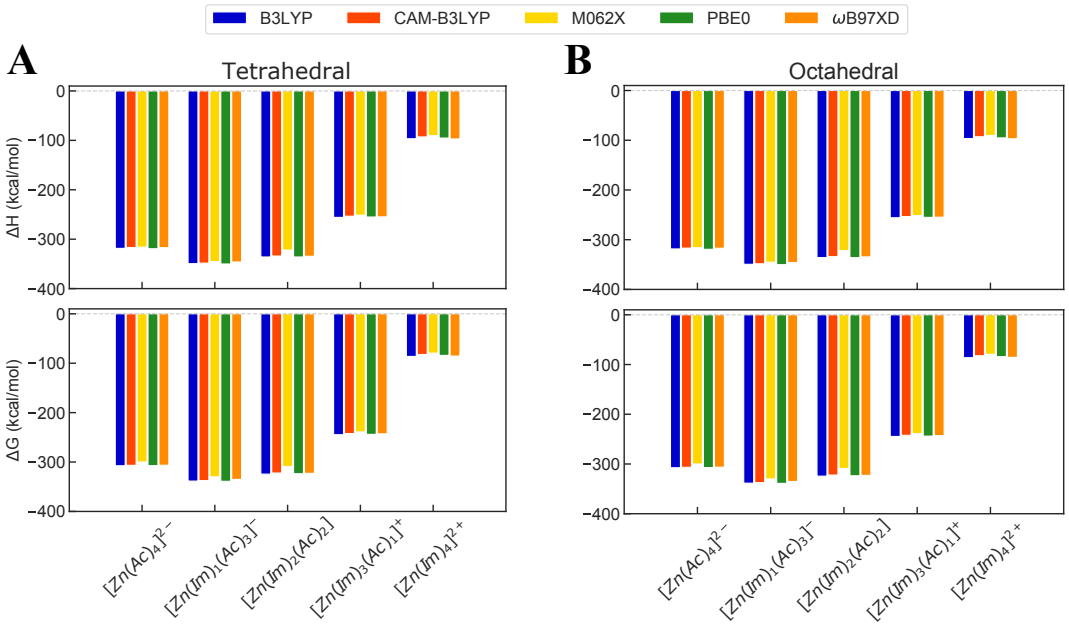

Figure S1: Comparison of the performance in of the different DFT functionals in the gas phase. Obtained ΔH and ΔG energies are shown for the FCS (A) and octahedral (B) clusters with all functionals.

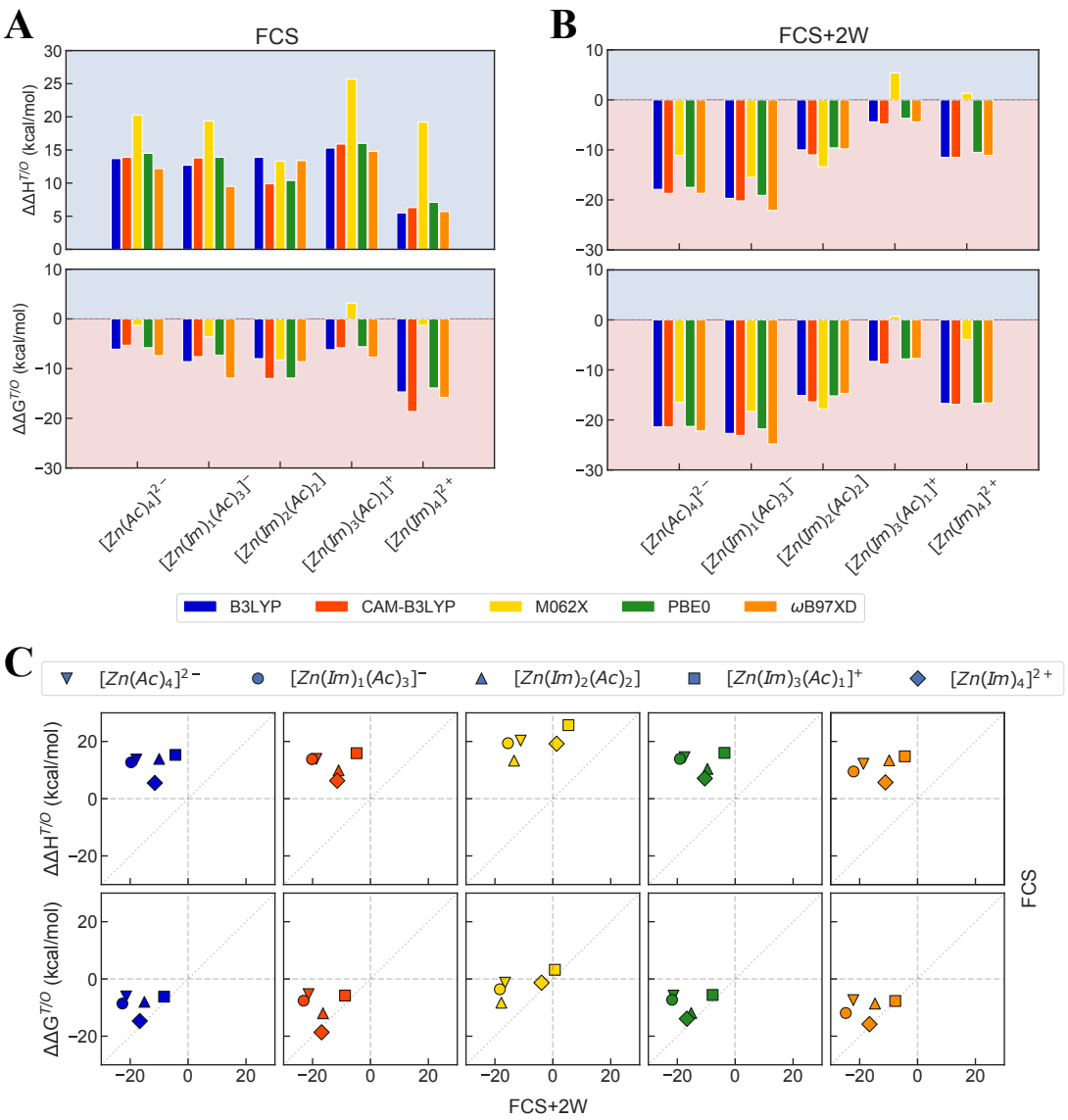

Figure S2: Comparison of the performance of the different DFT functionals in the gas phase. Obtained $\Delta\Delta H^{T/O}$ and $\Delta\Delta G^{T/O}$ energies are shown for the FCS (A) and FCS+2W (B). Correlation between the relative stabilities obtained with the different approaches (C) are also shown.

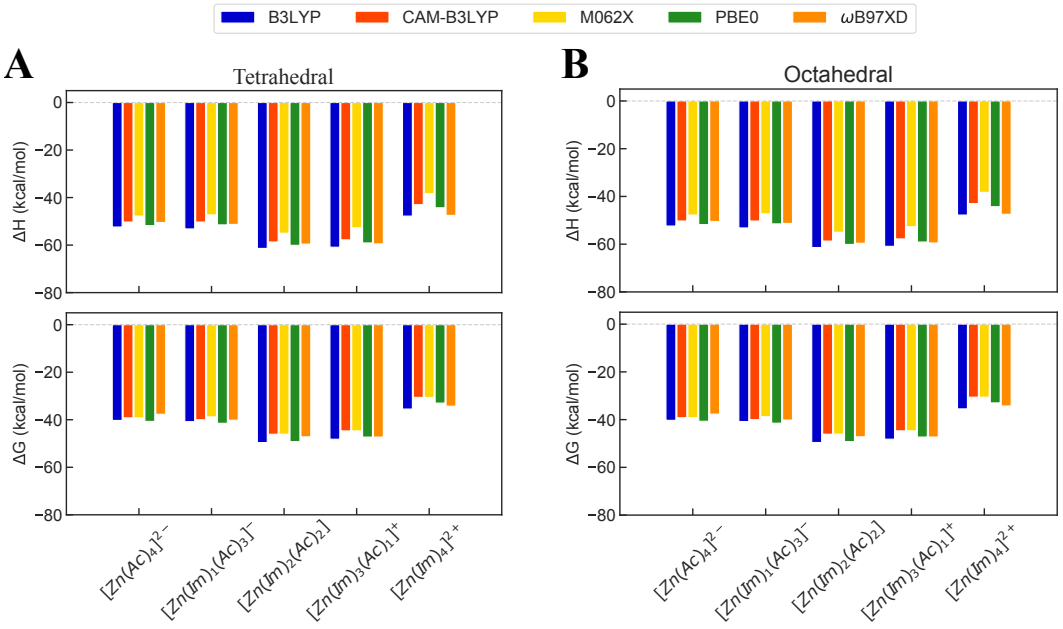

Figure S3: Comparison of the performance of the different DFT functionals in the solvent phase. Obtained ΔH and ΔG energies are shown for the FCS (A) and octahedral (B) clusters with all functionals.

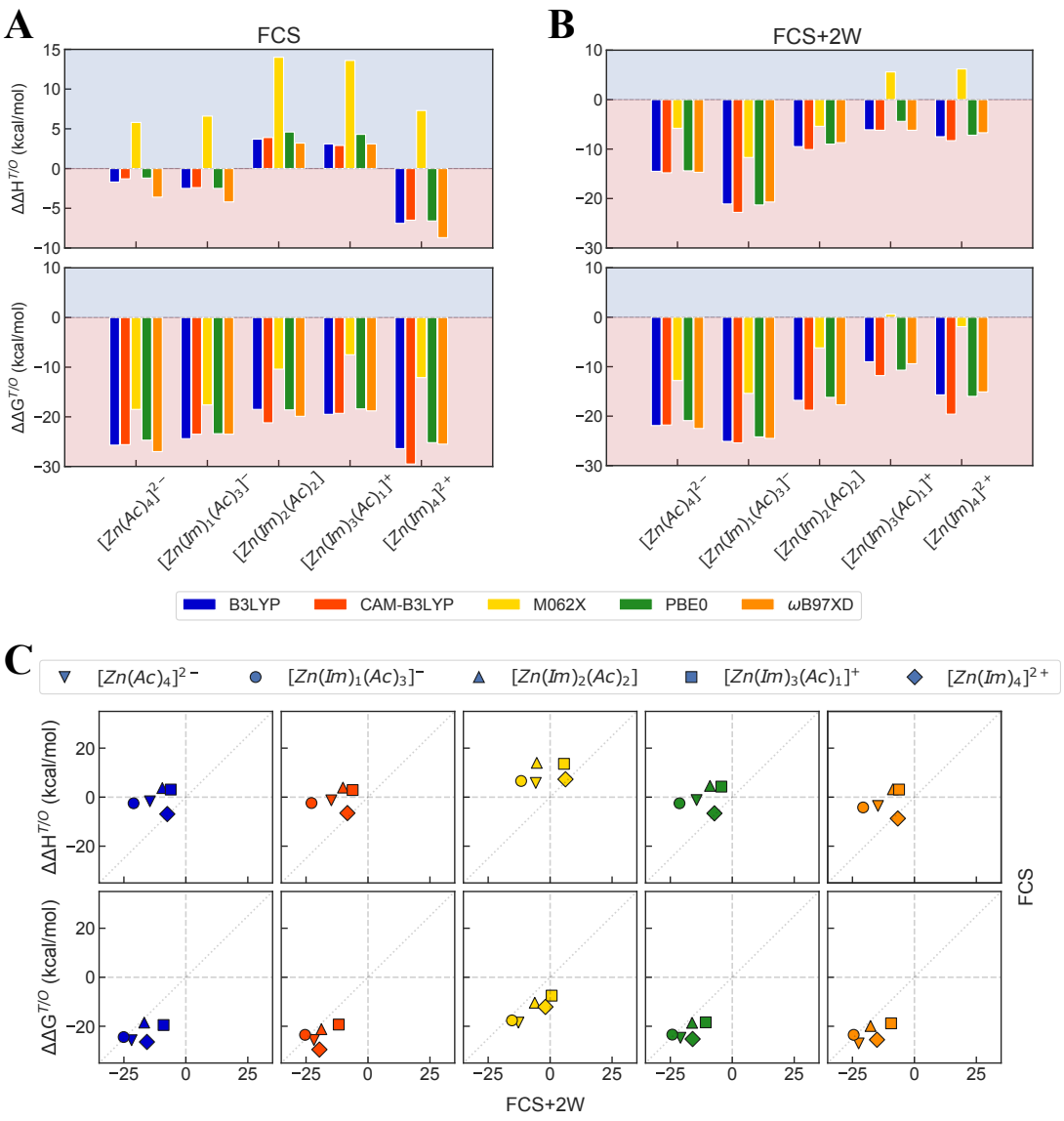

Figure S4: Comparison of the performance of the different DFT functionals in the solvent. Obtained $\Delta\Delta H^{T/O}$ and $\Delta\Delta G^{T/O}$ energies are shown for the FCS (A) and FCS+2W (B). Correlation between the relative stabilities obtained with the different approaches (C) are also shown.

II. RELATIVE STABILITIES OF Aβ-ZN(II) METAL CENTERS

In order to correct the energies obtained for the FCS+2W approach, we have calculated the ΔH^{OS} and ΔG^{OS} energies. Additionally, to calculate the corrected $\Delta\Delta H^{T/O}$ and $\Delta\Delta G^{T/O}$ energies, we have followed the scheme below

$$\Delta\Delta H^{T/O}_{corr} = \Delta\Delta H^{T/O} + \Delta H^{OS}$$
$$\Delta\Delta G^{T/O}_{corr} = \Delta\Delta G^{T/O} + \Delta G^{OS}$$

Table S1: Overstabilization introduced by the waters in the second coordination shell of tetrahedral clusters, $\Delta\Delta H^{T/O}_{corr}$ and $\Delta\Delta H^{T/O}_{corr}$ obtained with the ωB97XD functional in the gas phase. All energies in kcal/mol.

Cluster	ΔH^{OS}	ΔG^{OS}	$\Delta\Delta H^{T/O}_{corr}$	$\Delta\Delta G^{T/O}_{corr}$
$[Zn(Im)(Ac)_4]^{2-}$	30.9	14.8	12.2	-7.4
$[Zn(Im)_1(Ac)_3]^{-}$	31.6	12.9	9.5	-11.9
$[Zn(Im)_2(Ac)_2]$	23.2	6.1	13.4	-8.6
$[Zn(Im)_3(Ac)_1]^{+}$	19.3	0	14.9	-7.7
$[Zn(Im)_4]^{2+}$	16.8	0.8	5.7	-15.8

III. EFFECT OF DIFFERENT DIELECTRIC ENVIRONMENTS

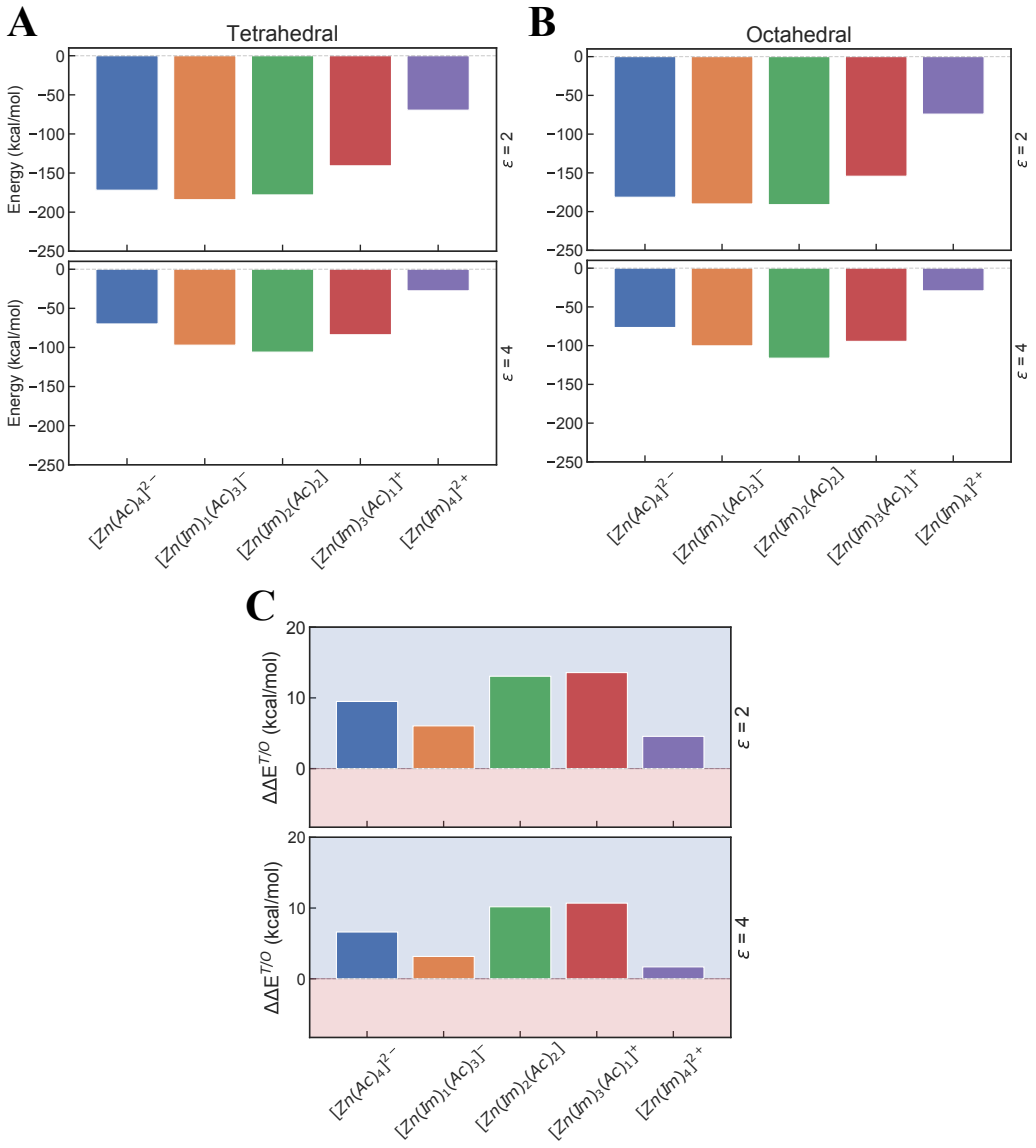

Figure S5: Energies of all tetrahedral (A) and octahedral (B) clusters at different dielectrics. Relative stabilities of the different coordination arrangements at different dielectrics (C). Results obtained with the ωB97XD functional.

IV. CONTRIBUTION OF EACH LIGAND

A. Ghost atom calculations

Table S2: ΔE_{Int}^{Zn}, ΔE_{f}^{CS}, ΔE_{Int}^{T}, E(2) and delocalization index of each ligand in tetrahedral clusters. Results obtained with the ωB97XD functional.

Cluster	Ligand	ΔE_{Int}^{Zn} (kcal/mol)	ΔE_{f}^{CS} (kcal/mol)	ΔE_{Int}^{T} (kcal/mol)	E(2) (kcal/mol)	Delocalization index (a.u.)
$[Zn(Ac)_4]^{2-}$	Ac1	-60.1	19.1	-41.0	-47.5	0.4285
	Ac2	-60.1	19.1	-41.0	-47.5	0.4281
	Ac3	-60.1	19.1	-41.0	-47.5	0.4284
	Ac4	-60.1	19.1	-41.0	-47.5	0.4282
$[Zn(Im)_1(Ac)_3]^{-}$	Im1	-49.8	10.6	-39.2	-57.7	0.4259
	Ac1	-59.1	14.6	-44.5	-46.8	0.4411
	Ac2	-58.4	14.4	-44.0	-45.3	0.4456
	Ac3	-60.8	17.3	-43.5	-49.3	0.4198
$[Zn(Im)_2(Ac)_2]$	Im1	-47.6	8.2	-39.4	-57.7	0.4632
	Im2	-50.1	8.1	-42.1	-60.3	0.4319
	Ac1	-67.2	17.6	-49.6	-49.7	0.4340
	Ac2	-59.7	15.2	-44.6	-43.2	0.4209
$[Zn(Im)_3(Ac)_1]^{+}$	Im1	-51.1	6.0	-45.0	-57.4	0.4340
	Im2	-50.6	8.2	-42.4	-61.1	0.4561
	Im3	-49.9	8.5	-41.3	-52.3	0.4392
	Ac1	-71.1	16.7	-54.4	-53.2	0.4479
$[Zn(Im)_4]^{2+}$	Im1	-55.7	5.9	-49.8	-60.8	0.4638
	Im2	-54.8	5.8	-48.9	-59.5	0.4588
	Im3	-56.2	6.1	-50.1	-61.5	0.4281
	Im4	-55.7	5.9	-49.8	-60.9	0.4583

Table S3: ΔE_{Int}^{Zn}, ΔE_f^{CS}, ΔE_{Int}^{T}, E(2) and delocalization index of each ligand in octahedral clusters. Results obtained with the ωB97XD functional.

Cluster	Ligand	ΔE_{Int}^{Zn} (kcal/mol)	ΔE_f^{CS} (kcal/mol)	ΔE_{Int}^{T} (kcal/mol)	E(2) (kcal/mol)	Delocalization index (a.u.)
$[Zn(Ac)_4(H_2O)_2]^{2-}$	Ac1	-54.3	15.8	-38.5	-47.1	0.3092
	Ac2	-49.2	12.4	-36.7	-40.8	0.3369
	Ac3	-52.2	14.6	-37.6	-42.6	0.3271
	Ac4	-49.6	14.7	-34.9	-38.8	0.3583
	Wat1	0.0	-10.8	-10.8	-12.2	0.1313
	Wat2	0.3	-11.3	-11.0	-12.0	0.1259
$[Zn(Im)_1(Ac)_3(H_2O)_2]^{-}$	Im1	-42.1	10.0	-32.1	-57.9	0.3561
	Ac1	-53.8	17.7	-36.1	-44.9	0.3367
	Ac2	-50.8	15.8	-34.9	-32.5	0.2916
	Ac3	-52.2	14.6	-37.6	-40.0	0.2906
	Wat1	-13.5	1.4	-12.1	-21.9	0.1938
	Wat2	-6.0	-5.9	-11.9	-18.5	0.1836
$[Zn(Im)_2(Ac)_2(H_2O)_2]$	Im1	-39.6	11.9	-27.7	-52.0	0.3330
	Im2	-40.0	11.1	-28.9	-51.4	0.3280
	Ac1	-67.4	15.3	-52.1	-41.1	0.3179
	Ac2	-58.9	13.1	-45.8	-41.3	0.2832
	Wat1	-20.5	-0.5	-21.0	-32.5	0.2608
	Wat2	-11.0	0.4	-10.6	-27.4	0.1700
$[Zn(Im)_3(Ac)_1(H_2O)_2]^{+}$	Im1	-43.9	10.3	-33.6	-52.7	0.3577
	Im2	-40.2	10.9	-29.4	-52.5	0.3332
	Im3	-40.2	9.9	-30.3	-53.0	0.3276
	Ac1	-58.7	9.2	-49.6	-38.2	0.2596
	Wat1	-16.3	3.2	-13.1	-34.3	0.2014
	Wat2	-20.2	-1.1	-21.3	-36.6	0.2454
$[Zn(Im)_4(H_2O)_2]^{2+}$	Im1	-43.7	8.5	-35.2	-53.2	0.3442
	Im2	-44.6	9.6	-35.0	-54.3	0.3522
	Im3	-42.4	9.6	-32.8	-50.9	0.3276
	Im4	-40.9	10.4	-30.5	-48.9	0.3056
	Wat1	-22.2	8.8	-13.4	-37.4	0.1895
	Wat2	-22.5	9.2	-13.2	-39.3	0.1823

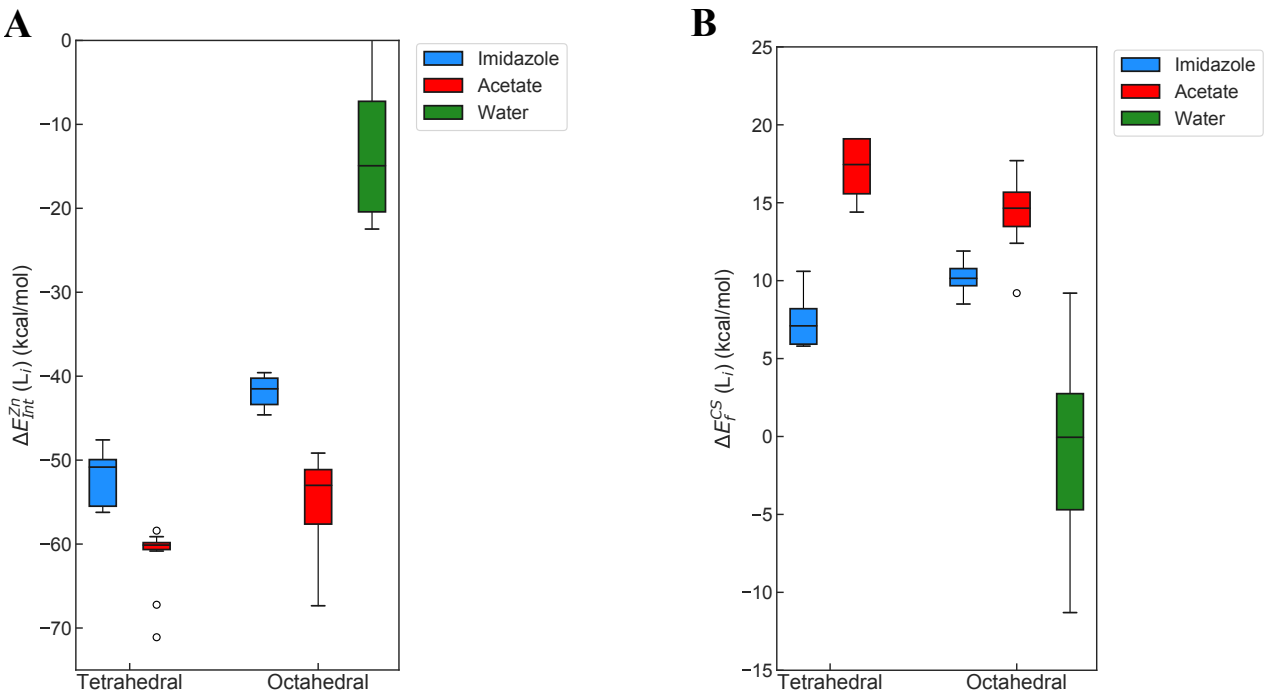

Figure S6: Results obtained using ghost atoms. Distribution of ΔE_{Int}^{CS} (A) and distribution of ΔE_{f}^{CS} (B). Results obtained with the ωB97XD functional.

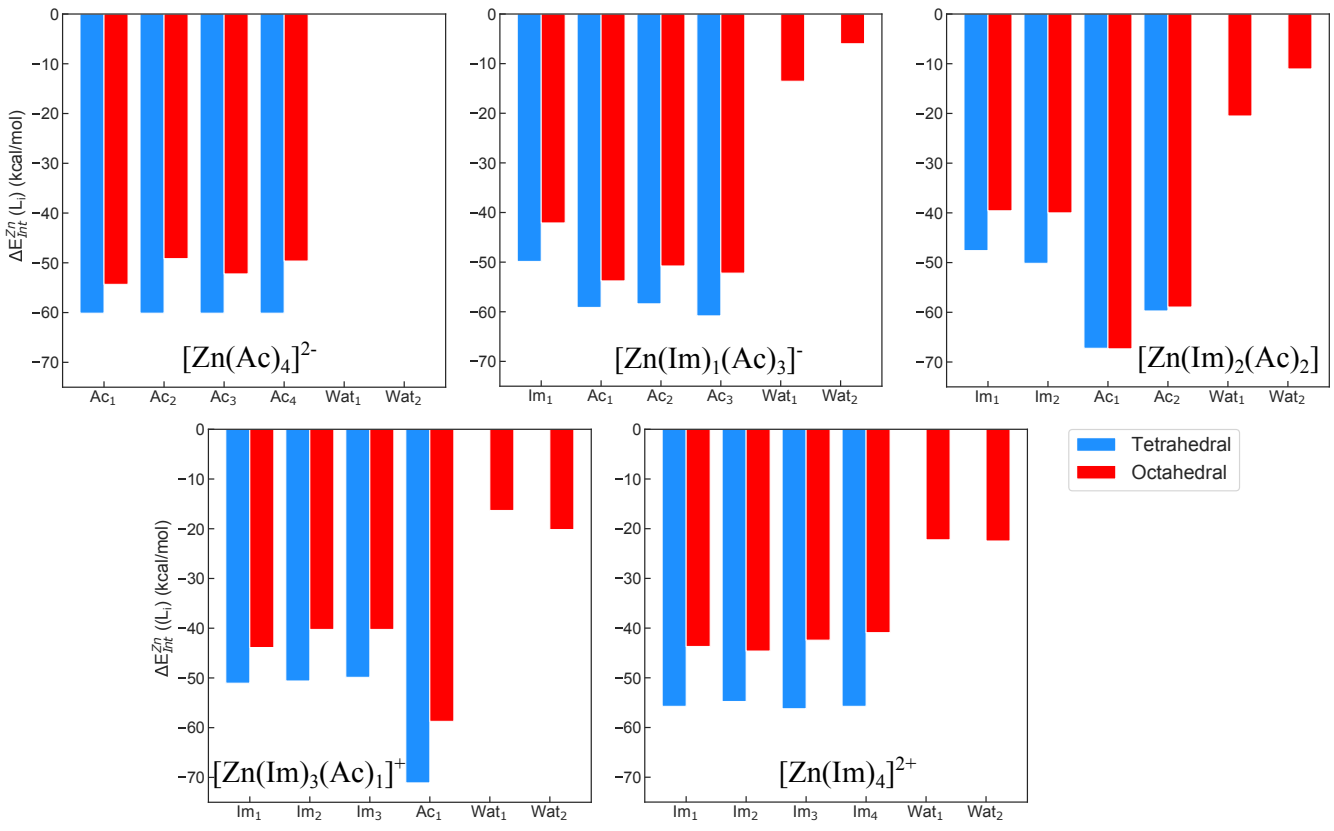

Figure S7: ΔE_{int}^{CS} energies obtained for each ligand in each cluster. Results obtained with the ωB97XD functional.

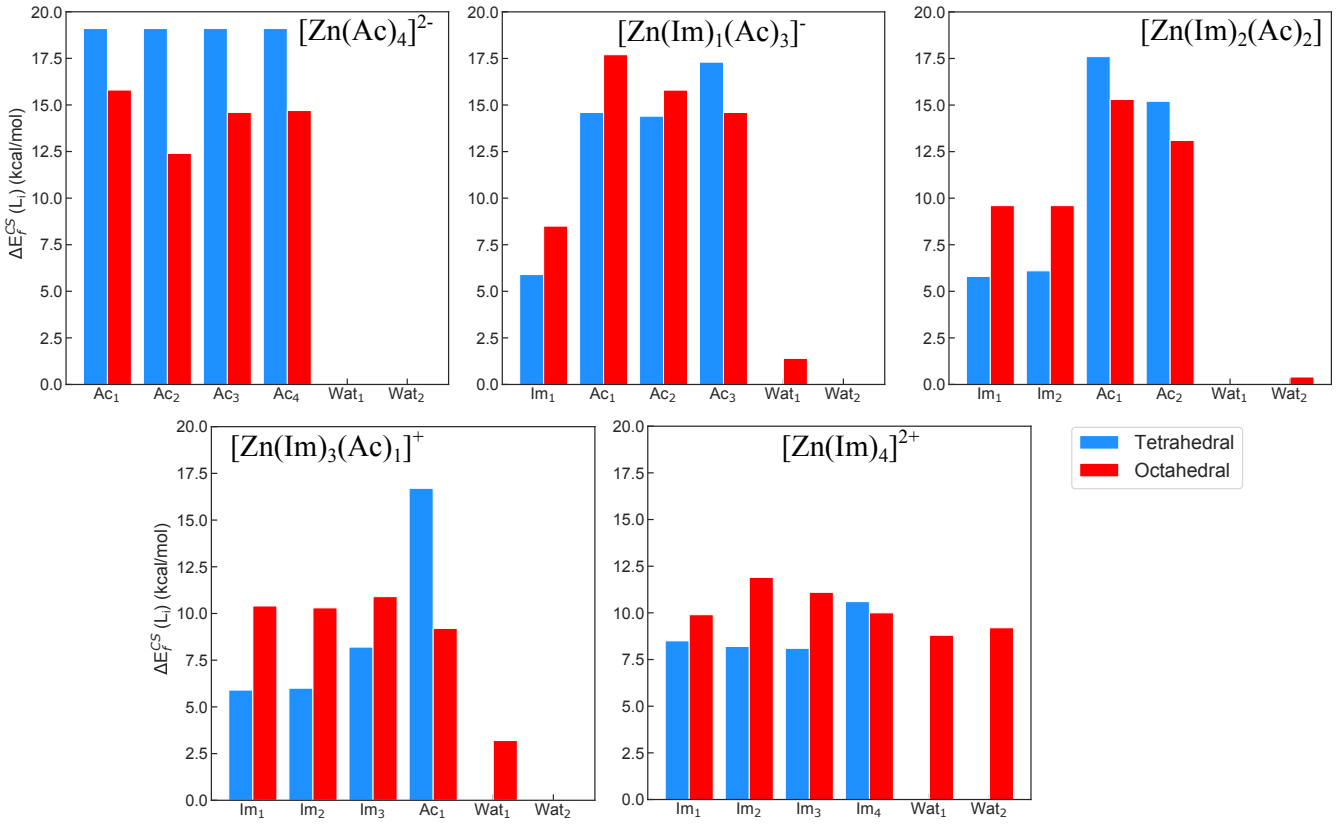

Figure S8: ΔE_f^{CS} energies obtained for each ligand in each cluster. Results obtained with the ωB97XD functional.

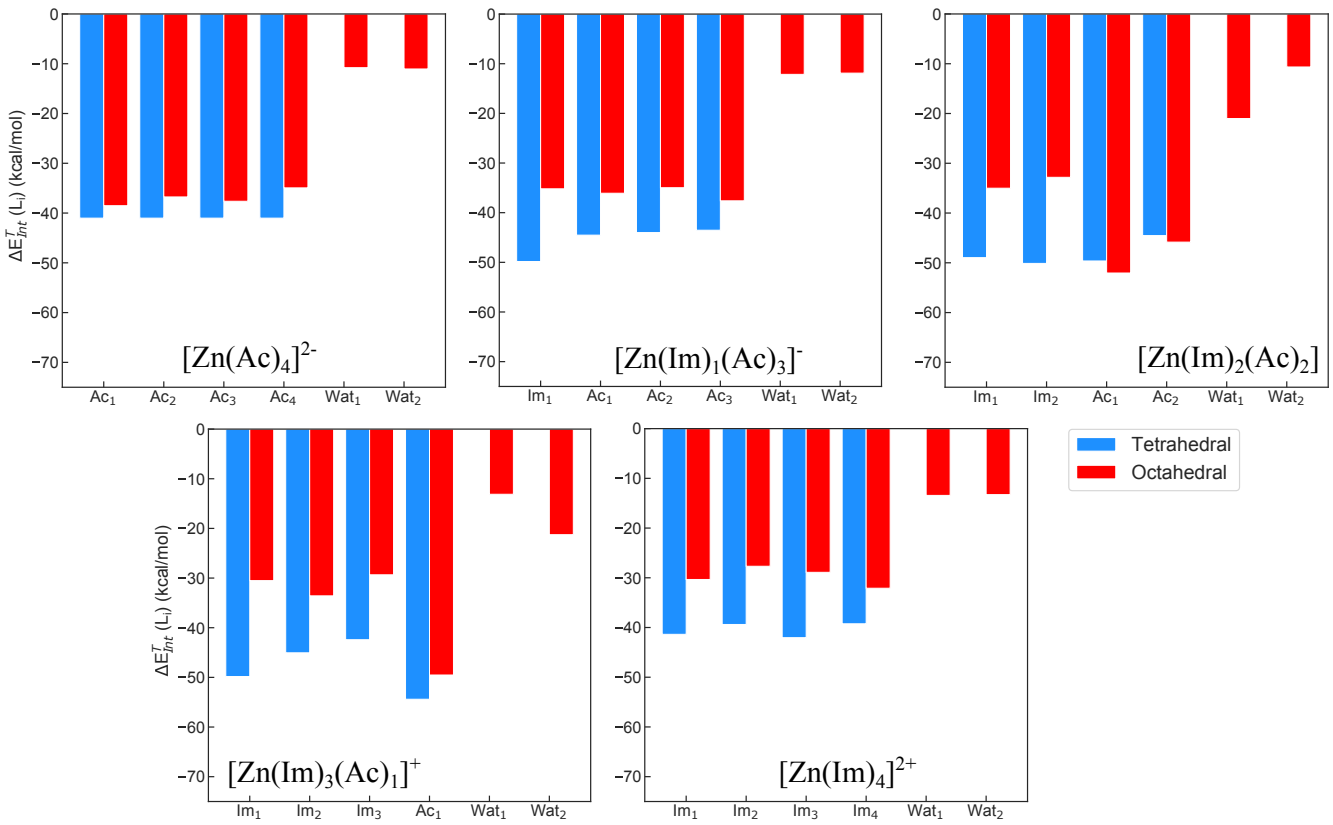

Figure S9: ΔE_{int}^{T} energies obtained for each ligand in each cluster. Results obtained with the ωB97XD functional.

B. Dative covalent interactions

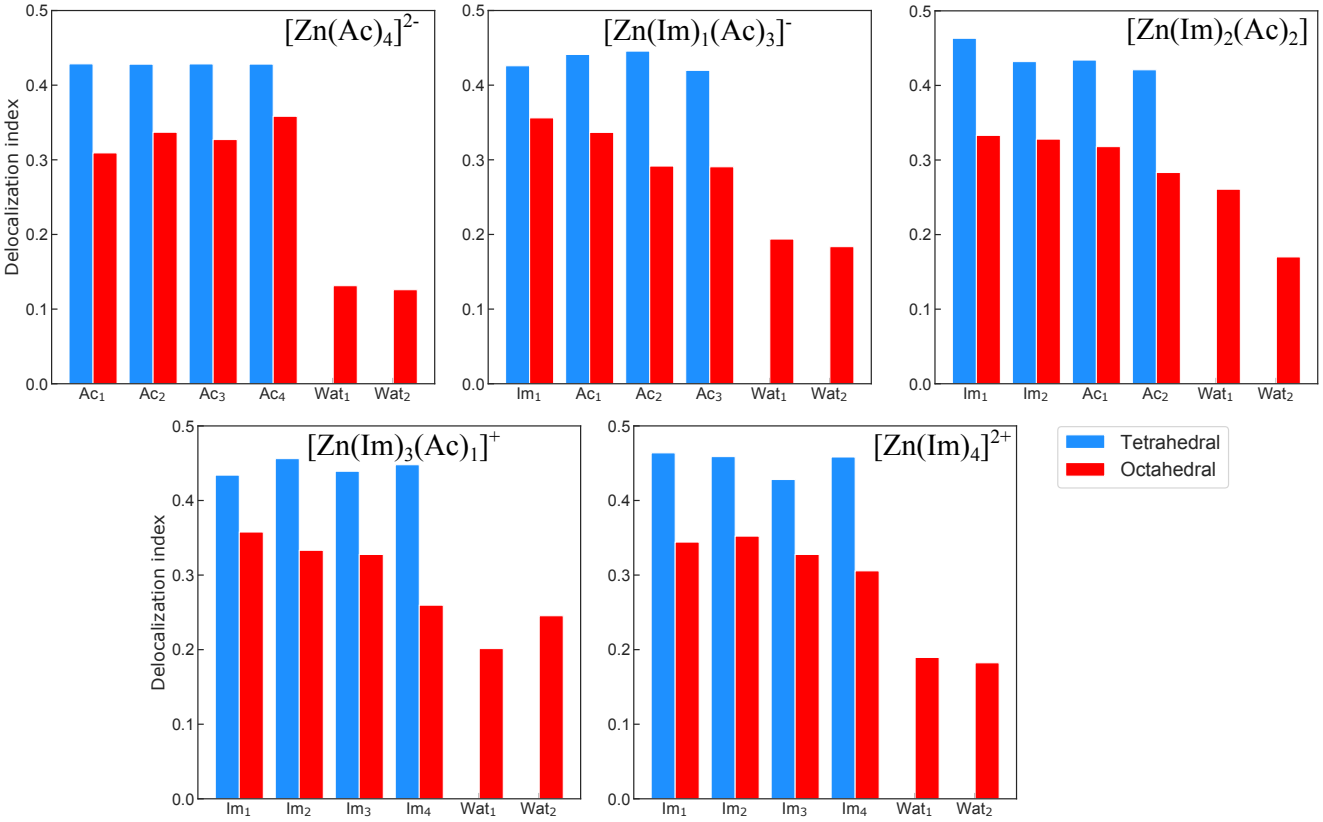

Figure S10: Delocalization index of each ligand in each cluster in a.u. Results obtained with the ωB97XD functional.

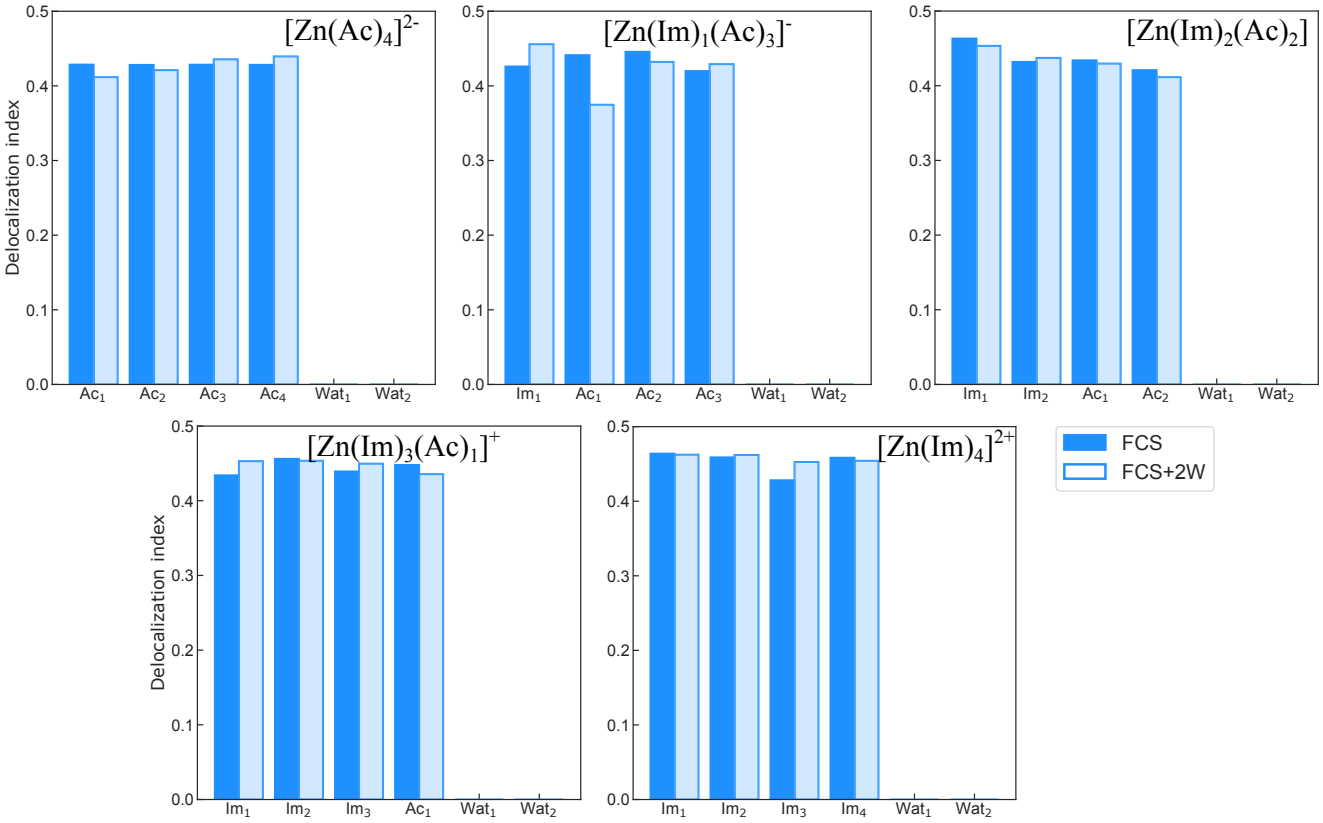

Figure S11: delocalization index of each ligand in each tetrahedral cluster in a.u. Results obtained with the ωB97XD functional.

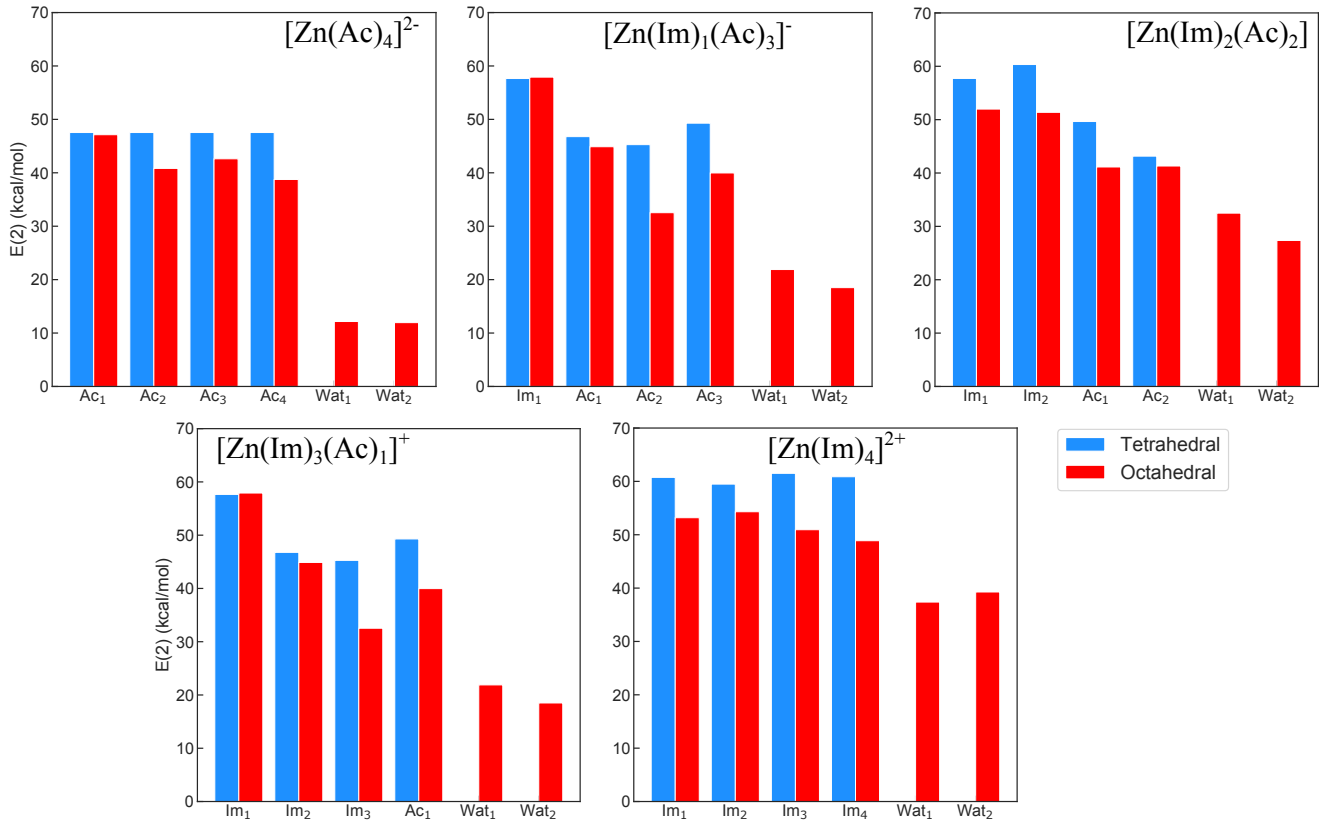

Figure S12: E(2) energies calculated for each ligand in each cluster. Results obtained with the ωB97XD functional.

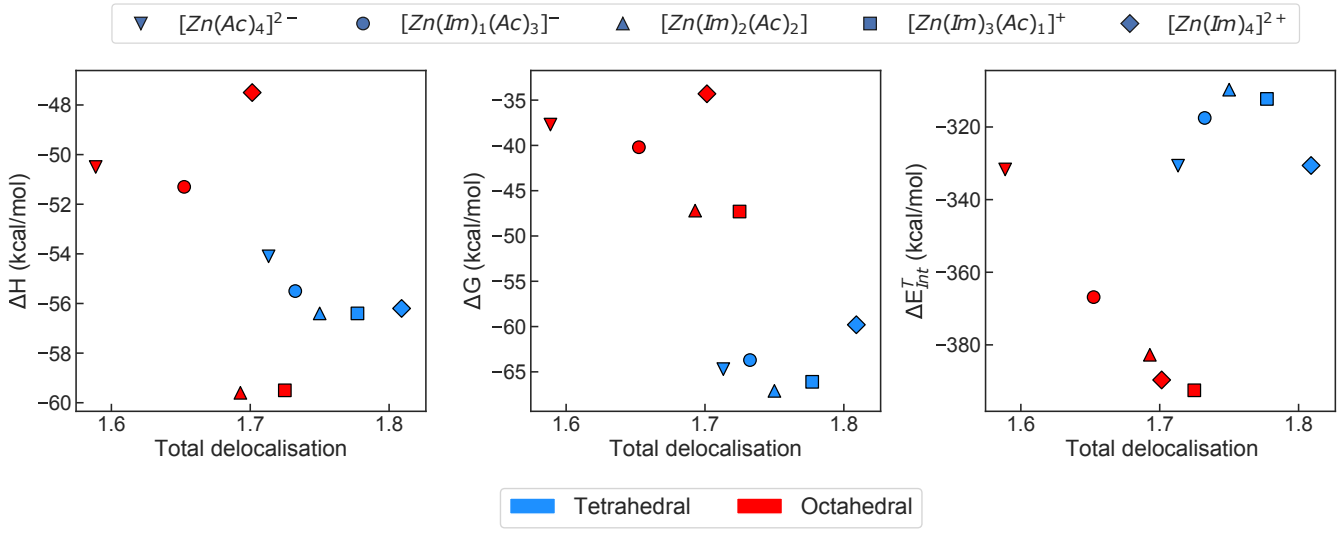

Figure S13: From left to right, correlation between total delocalization and ΔH, ΔG and ΔE_{Int}^{T} respectively. Results obtained with the ωB97XD functional.

C. Electrostatic interactions

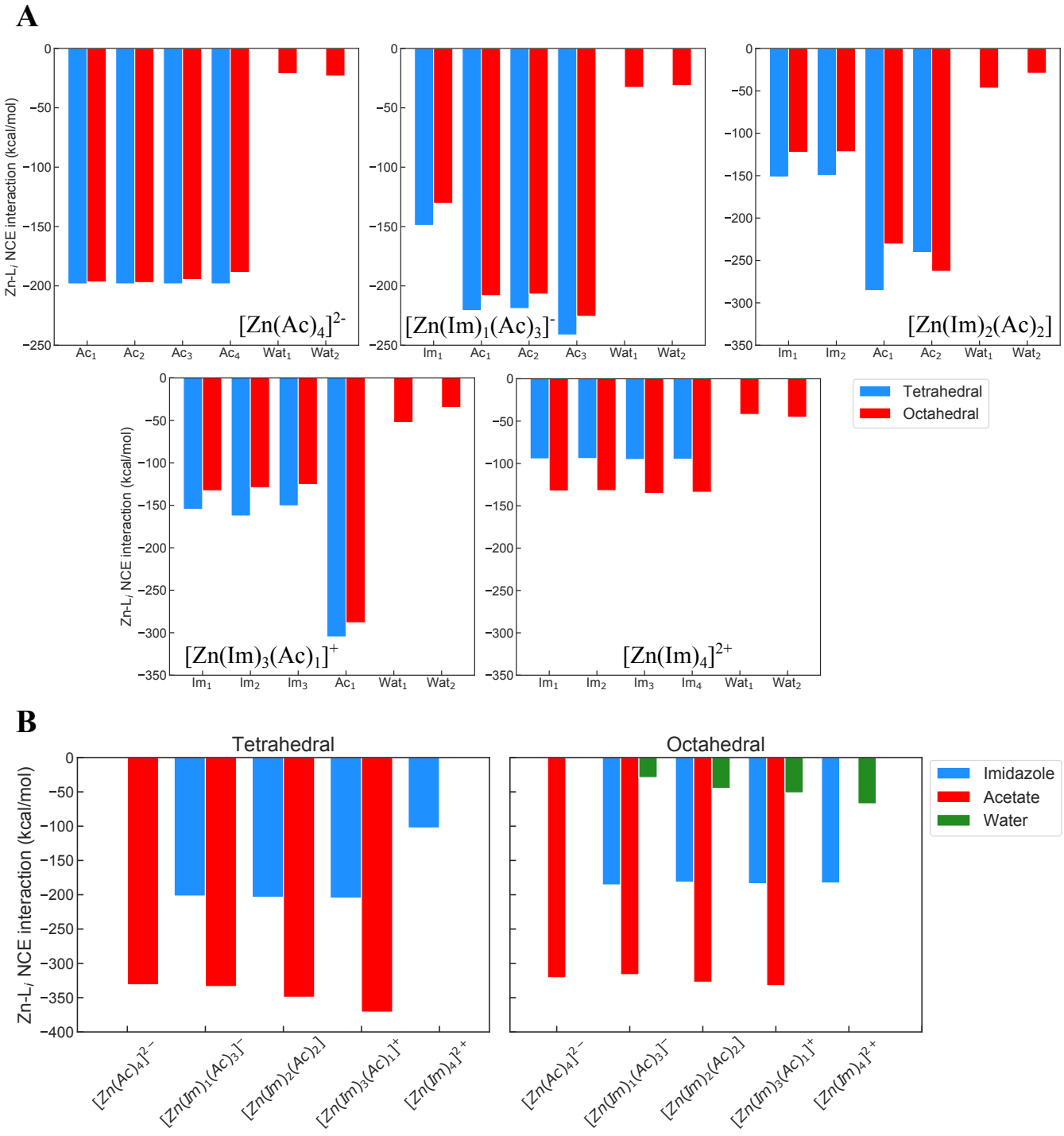

Figure S14: Zn-L$_i$ NCE interaction calculated using Lewis charges. Zn-L$_i$ NCE interaction of each ligand in each cluster (A) and average Zn-L$_i$ NCE interactions of acetates and imidazoles in each cluster (B). Results obtained with the ωB97XD functional.

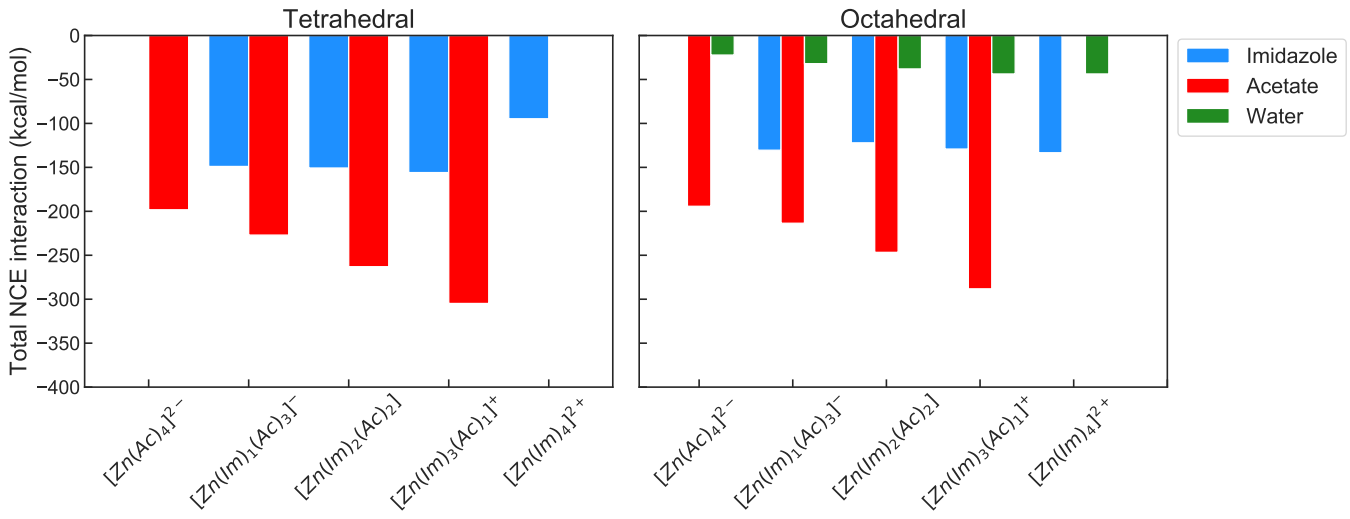

Figure S15: Total NCE interaction calculated using Lewis charges. Results obtained with the ωB97XD functional.

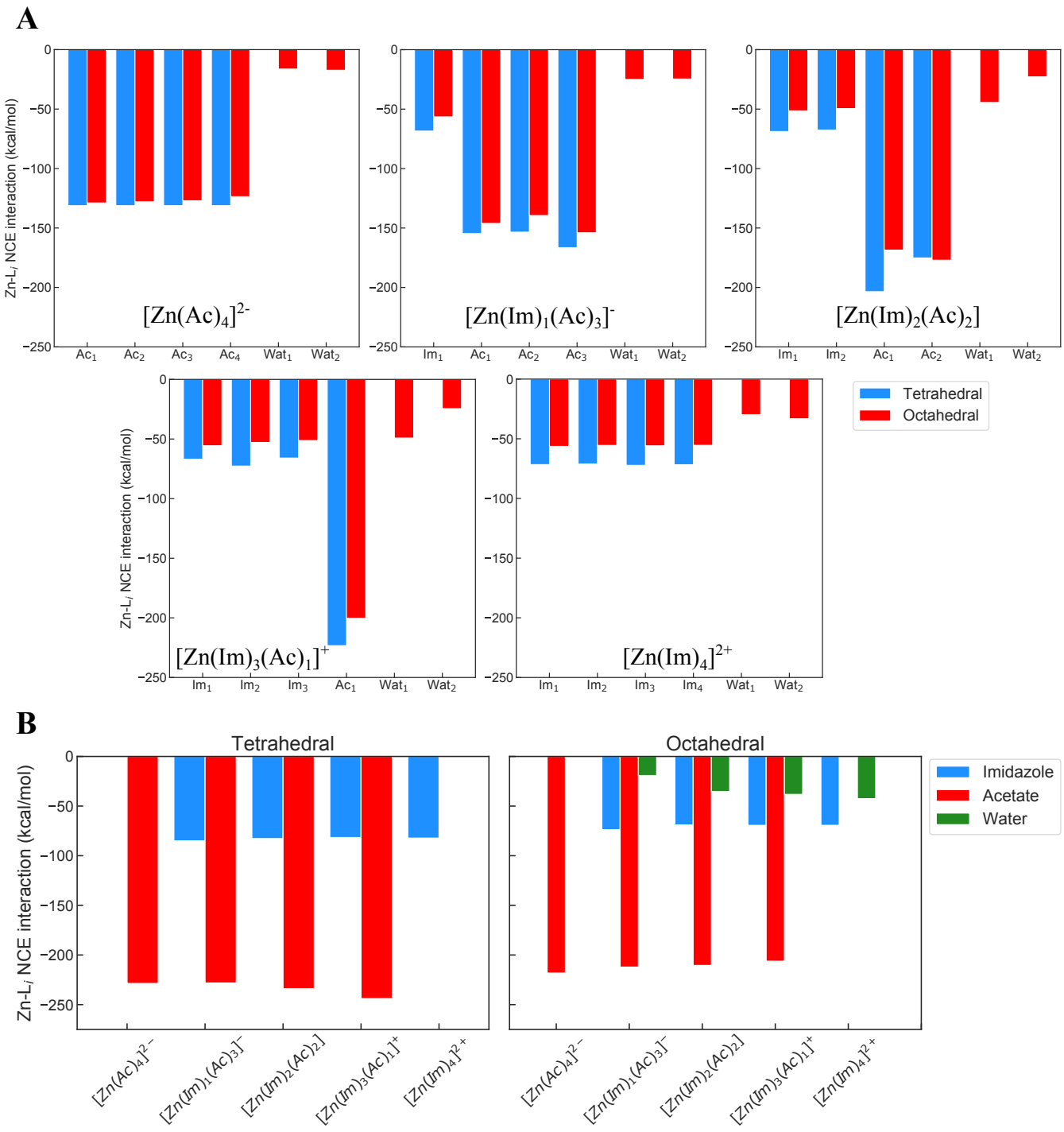

Figure S16: Zn-L$_i$ NCE interaction calculated using Non-Lewis charges. Zn-L$_i$ NCE interaction of each ligand in each cluster (A) and average Zn-L$_i$ NCE interactions of acetates and imidazoles in each cluster (B). Results obtained with the ωB97XD functional.

V. SELECTION OF PROTONATION STATE OF HISTIDINES

Histidines are known to adopt different protonation states when coordinating to metals, hisitidines with protons in the δ N being called HIS-D or HID and histidines with protons in the ε N being called HIS-E or HIE. In this study, the reduced models of histidines were built considering all histidines were protonated in the ε N. This decision was taken after ensuring that both type of histidines, HID and HIE, give the same values to the different calculations performed. To test the equivalence of both histidine types, we directly used the PDB ID 1ZE9 model [1] to build our system, which we show in orange in Figure S17. The 1ZE9 model was selected as two of the three histidines coordinating Zn(II) are protonated in the ε N (His6 and His14, Im1 and Im3, respectively) and one protonated in the δ N (His13, Im2). As shown in Figure S17, after comparing the results obtained with the model we built with the model built from the PDB model, we see the same exact tendencies and values are obtained for imidazoles in different protonation states.

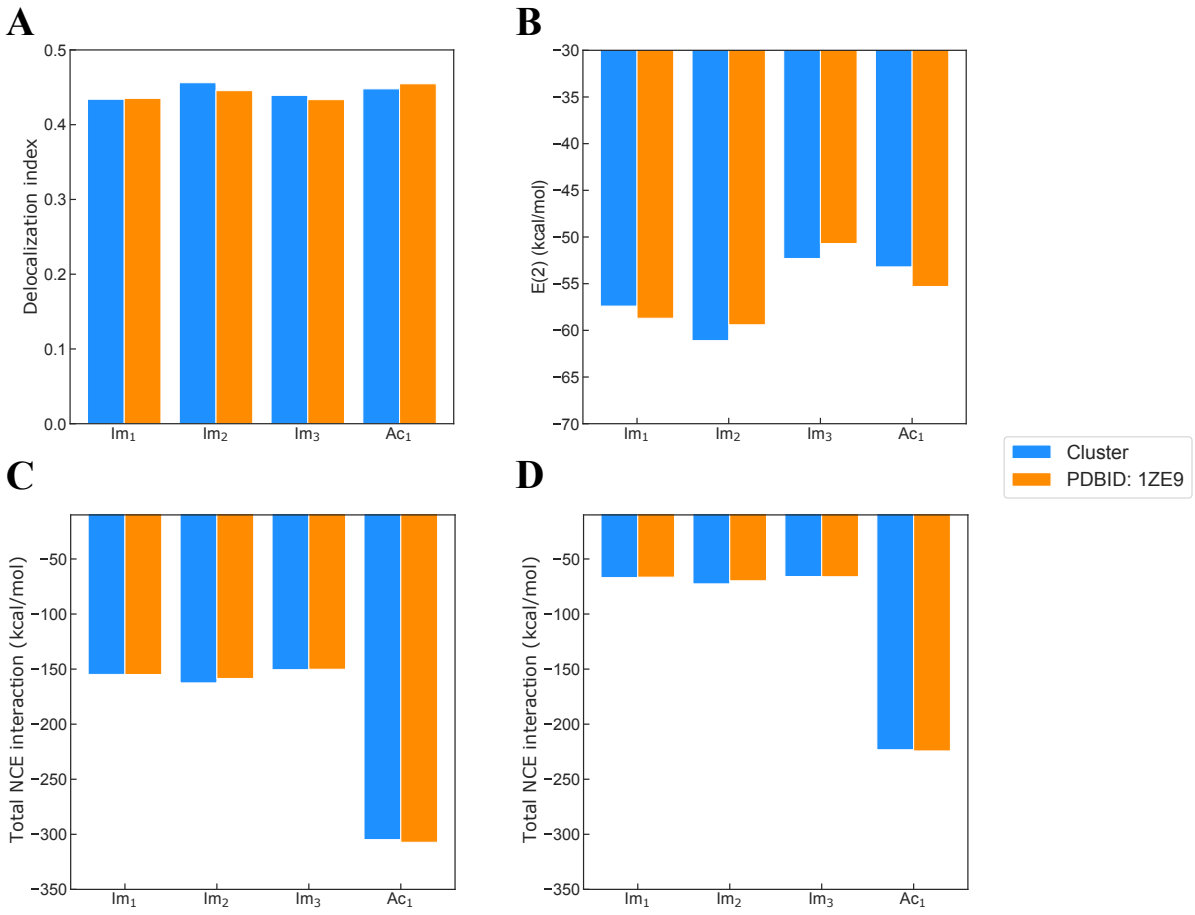

Figure S17: Results obtained for the tetrahedral cluster with all HIE histidines and results obtained for the PDBID 1ZE9 metal centre, where delocalization indexes (in a.u.) (A), E(2) energies obtained from NBO (B) and total NCE interactions obtained with Lewis charges (C) and Non-Lewis charges (D) are shown. Results obtained with the B3LYP functional.

VI. ENZYME-ZN(II) COORDINATION

Table S4: Number of the most common coordination spheres listed per-enzyme. Total number of coordination spheres sums up to the total number of coordination shells listed for each enzyme.

Coordination sphere	Oxidoreductase	Hydrolase	Lyase	Isomerase
S-S-S-S	106	129	-	9
Im-Im-Im-Ac^-	51	116	17	5
Im-Im-Ac^--Ac^-	8	98	12	22
Im-Ac^--Ac^--Ac^-	-	-	-	8
Total count of coordination spheres	303	1452	186	55

[1] S. Zirah, S. A. Kozin, A. K. Mazur, A. Blond, M. Cheminant, I. Ségalas-Milazzo, P. Debey, and S. Rebuffat, J. Biol. Chem. **281**, 2151 (2006).